

Late-time photometry of two nearby type II-P supernovae: 2004dj and 2004et *

Tian-Meng Zhang^{1,2,4}, Xiao-Feng Wang^{3,5}, Xu Zhou¹, Jun Ma¹, Zhao-Ji Jiang¹,
Jiang-Hua Wu¹, Zhen-Yu Wu¹ and Stéphane Basa²

¹ National Astronomical Observatories, Chinese Academy of Sciences, Beijing 100012, China;
armengjade@gmail.com

² Observatoire Astronomique de Marseille-Provence, 38, rue Fric Joliot-Curie, 13388 Marseille
Cedex 13, France

³ Physics Department and Tsinghua Center for Astrophysics (THCA), Tsinghua University, Beijing
100084, China

⁴ Graduate University of Chinese Academy of Sciences, Beijing 100049, China

⁵ Department of Astronomy, University of California, Berkeley, CA 94720-3411, USA

Received 2008 October 31; accepted 2009 March 19

Abstract We present late-time photometry for two bright type II-P supernovae (SNe) 2004dj and 2004et, extending over 400 d after the explosion, which are measured with a set of intermediate-band filters that have the advantage of tracing the strength variations of some spectral features. Although these two SNe II-P exhibit similar photometric evolution at earlier times, they diverge during the nebular phase. SN 2004dj shows a slow late-time decline rate with $\sim 0.7 \pm 0.1 \text{ mag (100 d)}^{-1}$ during the period ranging from $t \approx 200 - 300 \text{ d}$ after the explosion, while SN 2004et shows a much faster decline rate at a comparable phase, e.g., $1.3 \pm 0.1 \text{ mag (100 d)}^{-1}$. The steeper decay rate seen in SN 2004et is likely due to dust formation in the explosion ejecta. Based on intermediate-band photometry, we derived the evolution of the feature lines [e.g., H α] of SNe 2004dj and 2004et which are similar in flux at comparable phases but perhaps with significantly different decay rates. The origin of the observed variations in the continuum and the feature lines is briefly discussed.

Key words: supernovae: general — supernovae: individual (SN 2004dj, SN 2004et) — techniques: photometric

1 INTRODUCTION

Supernovae (SNe) fall into two primary categories: SNe Ia arise from the thermonuclear explosion of accreting carbon-oxygen (C-O) white dwarfs (WDs) with masses close to the Chandrasekhar limit ($\sim 1.4 M_{\odot}$) in a binary system; SNe II come from massive stars ($\geq 8 M_{\odot}$) which undergo core collapse and subsequent ejection of their hydrogen-rich envelopes and develop iron cores. As one subclass of core-collapse SNe, the progenitors of SNe II-P were thought to be massive stars with main-sequence masses less than $25 M_{\odot}$ (Li et al. 2007; Smartt et al. 2009).

Observationally, SNe II-P are distinguished by the presence of prominent hydrogen lines in their spectra, and their light curves are characterized by a plateau phase after a maximum which is formed

* Supported by the National Natural Science Foundation of China.

when the photosphere gradually recedes through the hydrogen envelope and the ionized hydrogen continuously recombines with the release of energy. Obviously, the length of the plateau depends on the depth of the hydrogen envelope, but other characteristics of the progenitors are also correlated with the plateau phase. In particular, the luminosity of the plateau is brighter for SNe II which produce more nickel, and both of these quantities are linked with higher explosion energies and ejecta velocities (Hamuy 2003). These correlations allow the standardization of SNe II-P luminosities to be around 0.3 mag through spectroscopic measurement of the ejecta velocities. This provides a distance measure to these objects independent of the Expanding Photosphere Method (EPM) (Schmidt et al. 1992; Leonard et al. 2002a), which may be applied to determine the cosmological parameters related to SNe Ia (Nugent et al. 2002).

With respect to plateau characteristics, studying the radioactive tail in the light curve is also interesting: it might also shed light on the explosion and provide additional constraints on their progenitors. In principle, nebular exponential decay is primarily controlled by radioactive decay of the newly synthesized materials during the SN explosion (Weaver & Woosley 1980); however, interaction of the SN ejecta with circumstellar material (CSM) and/or light echo may also shape the light curve during the nebular phase, which was evidenced in SNe Ia (e.g., Wang et al. 2008). The tail photometry of SNe II-P is usually difficult to obtain due to the sharp decrease of the luminosity from the plateau phase by 2 – 3 mag. The two nearby, bright type II-P SNe 2004dj and 2004et allow very late-time observations.

SN 2004dj was discovered by K. Itagaki (Nakano et al. 2004) on 2004 July 31.76 (UT time is used throughout the paper) in the nearby SBcd galaxy NGC 2403 at a distance of 3.3 ± 0.1 Mpc (Karachentsev et al. 2004). The optical position was measured to be R.A. = $07^{\text{h}}37^{\text{m}}17^{\text{s}}.04$, Dec = $+65^{\circ}35'57''.84$ (J2000.0). The research of both Maíz-Apellániz et al. (2004) and Wang et al. (2005) shows that the position of this supernova is coincident with a compact star cluster (Sandage star 96, hereafter S96; Sandage 1984). In our first paper (Zhang et al. 2006), we presented the early-time photometry of SN 2004dj and estimated the explosion date, the reddening, the synthesized ^{56}Ni mass, and some explosion parameters. SN 2004et was discovered by S. Moretti (Zwitter et al. 2004) on 2005 September 27 in the SABcd galaxy NGC 6946, with a reported position of R.A. = $25^{\text{h}}35^{\text{m}}25^{\text{s}}.33$, Dec = $+60^{\circ}07'17''.7$, (J2000.0). This galaxy is an amazing SN producer which recorded nine SNe (SNe 1917A, 1939C, 1948B, 1968D, 1969P, 1980K, 2002hh, 2004et, and SN 2008S) in the past century. The adopted distance to NGC 6946 is 5.5 ± 1.0 Mpc from the H I Tully-Fisher relation (Pierce 1994; Li et al. 2005 and references therein).

This paper is organized as follows. The observations and data reduction are described in Section 2, and the multicolor light curves are presented in Section 3. Discussions and conclusions are given in Section 4.

2 OBSERVATIONS AND DATA REDUCTION

We obtained the late-time light curves of these two bright Type II-P supernovae by the 60/90 cm Schmidt telescope located at the Xinglong station of the National Astronomical Observatories of China (NAOC). This system has a Ford Aerospace $2\text{K} \times 2\text{K}$ CCD camera with a 15 micron pixel size mounted at the Schmidt focus of the telescope. The field of view of the CCD is $58' \times 58'$ with a plate scale of 1.7 arcsec per pixel¹. Compared with the conventional broad-band Johnson-Cousins *UBVRI* system, this telescope is characterized by a photometric system with 15 intermediate-band (with FWHM $\approx 200 - 400$ Å) filters covering a wavelength range from 3000 Å to 10000 Å (Fan et al. 1996; Yan et al. 2000; Zhou et al. 2003). This photometric system, also dubbed the BATC system, was used to conduct a survey project among astronomers in Beijing, Arizona, Taipei, and Connecticut (Fan et al. 1996), and was designed to avoid contamination from the strongest and most variable night sky emission lines. The BATC system defines the magnitude zero points in a way similar to the spectrophotometric AB magnitude system, and is based on the SEDs of the four F sub-dwarfs, HD 19445, HD 84937, BD+262606, and

¹ A new $4\text{K} \times 4\text{K}$ CCD has been used in this telescope from 2007 so that the field of view increased to $1.5^{\circ} \times 1.5^{\circ}$ with a spatial resolution of 1.3 arcsec per pixel.

BD+174708 (Oke & Gunn 1983). The transformation equations between intermediate-band photometry and broadband *UBVRI* photometry are described by Zhou et al. (2003).

As the early-photometry of SNe 2004dj and 2004et has been presented elsewhere (Zhang et al. 2006; Sahu et al. 2006; Vinkó et al. 2006; Tsvetkov et al. 2008), in this paper, we focus on the late-time light curves of these two type II-P SNe. Since our photometric passbands are intermediate in size and the transmission curves are essentially flat in each band, we can also gain knowledge about the evolution of some emission lines from our unique intermediate-band photometry (Zhang et al. 2004; Zhang et al. 2006).

As supernovae usually explode near the spiral arms and/or the H II regions of the host galaxy, their photometry is usually more complicated and relies on specific techniques such as template subtraction. The template images of the SN 2004dj field (NGC 2403) were fortunately obtained prior to its burst during the Multi-color Sky Survey of BATC since 1995 (Wang et al. 2005). This allows us to perform image subtraction to remove the contamination of a compact star cluster (S96; Sandage 1984 with $V \sim 18.0$ mag. Template images prior to the burst of SN 2004et are, however, unavailable. To obtain proper photometry for this SN, we applied a method to fit the background underneath the SN by resolving the Laplace equation (Zhang et al. 2004).

The final step is to perform standard aperture photometry on the subtracted images of SNe 2004dj and 2004et. We used Pipeline II (a program developed to measure the magnitudes of point sources in BATC images) that is based on Stetson's DAOPHOT package (Stetson 1987). The final magnitudes of these two SNe II-P are listed in Tables 1 and 3, respectively. The errors shown in parentheses are a quadrature sum of the uncertainties in photometry and the calibrations.

Table 1 Late-time Photometric Data of SN 2004dj

Date (UT)	JD	<i>d</i>	<i>e</i>	<i>i</i>	<i>k</i>	<i>m</i>
08/01/05	2453387	14.18(01)	15.27(04)	15.15(04)
09/01/05	2453388	...	15.76(08)	14.13(04)	...	15.25(03)
19/01/05	2453390	...	15.92(05)	14.20(01)
20/01/05	2453391	16.30(05)	15.22(03)	...
04/02/05	2453406	16.32(13)	15.60(05)	14.27(01)
07/02/05	2453409	...	15.81(05)	14.24(01)	...	15.28(04)
11/02/05	2453413	16.56(13)	...	14.31(01)
12/02/05	2453414	...	15.99(05)	...	15.46(04)	15.34(03)
16/02/05	2453418	16.56(10)	...	14.34(01)	...	15.42(05)
18/02/05	2453420	...	16.08(13)	14.37(02)
19/02/05	2453421	...	15.80(10)	14.42(02)	15.78(12)	15.60(09)
20/02/05	2453422	16.22(13)	16.25(14)	14.33(02)	...	15.29(07)
09/03/05	2453439	...	16.18(06)	14.48(02)
14/03/05	2453444	...	16.30(07)	14.49(03)	...	15.64(10)
16/03/05	2453446	...	16.08(12)	14.49(02)	...	15.53(10)
17/03/05	2453447	15.60(15)	...
19/03/05	2453449	17.13(34)	16.28(26)	14.55(03)	15.59(10)	...
22/03/05	2453452	...	16.27(23)	14.64(06)	...	15.75(11)
25/03/05	2453455	14.59(02)	15.67(10)	...
17/08/05	2453600	17.26(50)	17.04(32)	16.13(10)	17.10(29)	...
21/09/05	2453635	17.48(48)	17.26(32)	16.55(11)

3 MULTICOLOR LATE-TIME LIGHT CURVES

3.1 Light Curves of SN 2004dj

The early time photometry of SN 2004dj was presented in Zhang et al. (2006). With the multi-band light curves and SEDs, we estimated some properties of SN 2004dj's progenitor, including the explosion date, mass of ^{56}Ni , etc. The decline rate after the plateau phase was consistent with the decay rate of ^{56}Co .

After that, we kept observations of SN 2004dj with the same system and obtained late-time photometry data for this paper.

Figure 1 shows late-time light curves of SN 2004dj in five intermediate-band filters, spanning $t \sim +220$ d to $t \sim +470$ d after the explosion (assuming an explosion date of JD 2453167; Zhang et al. 2006). Overplotted are the data obtained in the early nebular phase (Zhang et al. 2006). The big gap between $t \approx 280 - 470$ d is due to the fact that the SN was behind the Sun during that period. The computed decline rates in different bands are listed in Table 2.

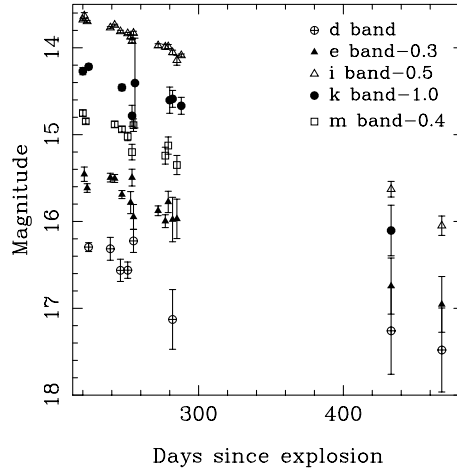


Fig. 1 Light curves of SN 2004dj in the BATC system.

Table 2 Decline Rate of Late-time Light Curve of SN 2004dj

Date since burst	<i>d</i> -band	<i>e</i> -band	<i>i</i> -band	<i>k</i> -band	<i>m</i> -band
220 – 280	0.69(28)	0.67(08)	0.60(02)	0.77(08)	0.67(09)
280 – 468	...	0.60(14)	1.07(05)	0.99(19)	...

One can see that the overall evolution in *d*, *e*, *k* and *m* filters is similar over $t \sim 220 - 280$ d, with an average decline rate of $\beta = 0.68 \pm 0.07$ mag $(100 \text{ d})^{-1}$, consistent with the determinations from our earlier analysis reported in Zhang et al. (2006). The exception is the evolution in the *i*-band, where the luminosity evolution seems to experience three stages: at $t = 140 - 220$ d, the *i*-band light curve nearly remained constant, then it declined at a rate comparable to the other bands during the period from $t = 220$ d to 280 d, and finally it likely decayed at a much faster pace after $t = 280$ d [e.g., $\beta = 1.07 \pm 0.05$ mag $(100 \text{ d})^{-1}$]. A similar steeper decay rate may hold in the *k*-band during $t = 280 - 470$ d, but there is a larger uncertainty in the measurement. Owing to poor data sampling, the decay rates in *d* and *m* during this phase are not given in Table 2.

The broadband photometry of SN 2004dj was obtained by Vinkó et al. (2006) and Tsvetkov et al. (2008), respectively, from which the decay rate in *BVRI* bands at $t \approx 200 - 300$ d was found to be $0.6-0.7$ mag $(100 \text{ d})^{-1}$, comparable to our intermediate-band determinations at a similar phase. With the very late-time data published by Tsvetkov et al. (2008), we further found that the slope of the *R*-band decay changed from 0.59 ± 0.03 mag $(100 \text{ d})^{-1}$ at $t \approx 200 - 300$ d to 0.82 ± 0.02 mag $(100 \text{ d})^{-1}$ at $t \approx 300 - 480$ d. This variance in slope is similar to that seen in the BATC *i*-band at a similar phase, though the change is smaller. This is because the *R*-band covered more continuum on either side of the H_{α} emission with respect to the BATC *i*-band.

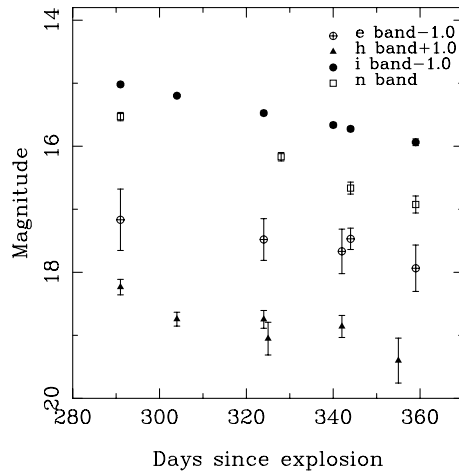


Fig. 2 Light curves of SN 2004et in the BATC system.

Table 3 Late-time Photometric Data of SN 2004et

Date(UT)	JD	<i>e</i>	<i>f</i>	<i>h</i>	<i>i</i>	<i>n</i>
15/07/05	2453567	19.69(47)	...	17.26(12)	16.95(04)	15.53(07)
28/07/05	2453580	17.76(11)	17.15(02)	...
17/08/05	2453600	19.92(31)	19.23(14)	17.80(16)	17.42(04)	...
21/08/05	2453604	16.17(07)
04/09/05	2453618	20.38(42)	19.47(17)	17.86(18)	17.60(04)	...
06/09/05	2453620	19.99(17)	17.68(04)	16.66(10)
17/09/05	2453631	18.25(32)
21/09/05	2453635	20.48(37)	19.66(17)	...	17.88(05)	16.92(14)
27/12/05	2453732	...	20.39(50)	19.40(70)

3.2 Light Curves of SN 2004et

The light curves of SN 2004et are shown in Figure 2. The observations were made in the *e*, *f*, *h*, *i*, and *n*-bands, spanning 291 to 359 d after the explosion with the assumption of the explosion date being September 22 2004 (JD 2453270.5; Sahu et al. 2006). The nebular-phase light curves generally declined in a linear fashion. The decay rates in the *e*, *f*, *h*, *i*, and *n* filters are estimated to be 0.94 ± 0.77 , 1.14 ± 0.54 , 1.18 ± 0.32 , 1.33 ± 0.06 , and 1.28 ± 0.11 (in units of $\text{mag} (100 \text{ d})^{-1}$), and the slope seems to become steeper towards longer wavelengths. Based on the broadband data reported in Sahu et al. (2006), we also derive the decay rates in *BVR**I*. This gives 0.79 ± 0.04 in *B*, 1.12 ± 0.03 in *V*, 1.22 ± 0.02 in *R*, and $1.33 \pm 0.02 \text{ mag} (100 \text{ d})^{-1}$ in *I*, respectively. One can see that the evolution in the broadband filters basically follows the trend seen in our intermediate bands.

4 DISCUSSIONS

4.1 Late-time Decay Rate

Since the SNe II-P light curves in the nebular phase are powered by the radioactive decay of $^{56}\text{Co} \rightarrow ^{56}\text{Fe}$, we should expect that their nebular-phase light curves decay at a rate $\sim 0.98 \text{ mag} (100 \text{ d})^{-1}$. The absolute *i*-band light curves of SNe 2004dj and 2004et are presented in Figure 3. In Table 4, we listed the exponential decaying rates as well as other important parameters of a few well-observed SNe II-P for comparison. In the nebular phase, most objects declined at a rate comparable to the decay rate of ^{56}Co . As presented in Section 3.1, however, SN 2004dj showed a slower decline rate with $\langle \beta \rangle =$

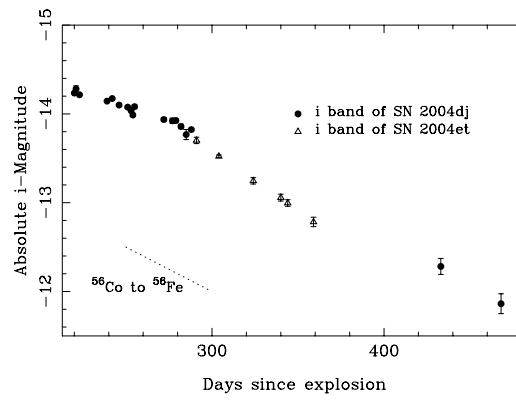


Fig. 3 Absolute *i*-band light curves of SN 2004dj and SN 2004et.

Table 4 Parameters of Some Well-observed SNe II-P

Supernova ¹	Distance (Mpc)	$E(B - V)$ (mag)	M_{Ni} (M_{\odot})	$M_{\text{Progenitor}}$ (M_{\odot})	M_V^{Plateau} (mag)	Decline Rate $\text{mag}(100 \text{ d})^{-1}$
SN 1990E	18^{+3}_{-2} b	$0.48^{+0.10}_{-0.10}$ a	0.073a	...	$-17.1^{+0.2}_{-0.4}$ a	0.93(12)a
SN 1997D	13.4h	0.00i	0.002g	26g	...	0.99(10)c
SN 1999em	$8.2^{+0.6}_{-0.6}$ c	$0.10^{+0.05}_{-0.05}$ d	0.09e	12f	$-15.9^{+0.2}_{-0.2}$ c	$1.12^{+0.06}_{-0.06}$ o
SN 2003gd	$9.3^{+1.8}_{-1.8}$ r	$0.14^{+0.06}_{-0.06}$ r	0.016r	8^{+4}_{-2} r	...	1.04(06)r
SN 2004A	$20.3^{+3.4}_{-3.4}$ q	$0.06^{+0.03}_{-0.03}$ q	$0.046^{+0.031}_{-0.017}$ q	12q	...	1.05(46)q
SN 2004dj	$3.47^{+0.29}_{-0.29}$ j	$0.33^{+0.11}_{-0.11}$ k	0.023l	12k	$-15.88^{+0.18}_{-0.18}$ j	0.68(07)p
SN 2004et	5.7m	0.41m	0.06m	15n	-17.14m	1.33(06)p

[1] SN 1990E, SN 1999em, SN 2004A, SN 2004dj and SN 2004et are all SNe II-P.

Reference: a) Schmidt et al. (1993); b) Schmidt et al. (1994); c) Benetti et al. (2001); d) Baron et al. (2000); e) Smartt et al. (2002); f) Leonard et al. (2003); g) Turatto et al. (1998); h) Tully (1988); i) RC3 catalogue; j) Wang et al. (2005); k) Vinkó et al. (2006); l) Zhang et al. (2006); m) Sahu et al. (2006); n) Li et al. (2005); o) Elmhamdi et al. (2003); p) This paper; q) Hendry et al. (2006); r) Hendry et al. (2005).

$0.68 \pm 0.07 \text{ mag} (100 \text{ d})^{-1}$, perhaps invoking additional energy apart from the radioactive decay. The possible sources responsible for this extra energy include interaction with the CSM, delayed optical input by finite recombination time, light echo and emission from a pulsar.

As radioactivity dominates the light curves at earlier epochs, either CSM interaction or light echo contribution will lead to a flatter evolution of the brightness at later epochs. This is not in accordance with the behavior seen in SN 2004dj which has a flatter light curve at earlier epochs (at $t = 220 - 280 \text{ d}$) and a steeper one at later epochs (at $t = 280 - 470 \text{ d}$). Nevertheless, the possibility of multiple CS shells around SN 2004dj might not be ruled out. The thermal emission from a young pulsar also appears an unlikely source, as pulsar emission is maintained for a long time and the pulsar photoionization nebula produces narrow emission lines ($\approx 1000 \text{ km s}^{-1}$; Chevalier & Fransson 1992). This is in contrast to the broad emission features seen in SN 2004dj's late-time spectra (e.g., Vinkó et al. 2006).

With respect to the other mechanisms discussed above, recombination emission might be more likely to contribute to the optical input of supernovae during the nebular phase because of longer recombination timescales, as suggested by Kozma & Fransson (1992). A quantitative analysis of the energy contribution from delayed recombination should be interesting but is beyond the scope of this paper.

In comparison with all the selected samples, we find that SN 2004et exhibited the fastest decline during the nebular phase. A steeper decay in the late-time light curve was also reported in SN 1987A (Catchpole et al. 1988) and 1999em (Elmhamdi et al. 2003), with a decline rate of 1.15 and 1.12 $\text{mag} (100 \text{ d})^{-1}$ at similar epochs, respectively. This suggests that during this phase either γ -ray leakage was

significant, or dust was formed in the supernova ejecta, or both of them occurred. Apart from the steepening of the decay rate of the optical light curves, the signature of dust formation includes flattening and blueshift of the emission peak of the [OI] doublet components at later epochs. This was observed in the late-time spectra of SN 2004et taken after 300 d since the explosion (Sahu et al. 2006). The newly formed dust grains may block some of the light from the supernova (Fransson et al. 2007) and result in the sudden dimming of the supernova beyond 300 d after the explosion. A similar signature of dust formation was also seen in the spectra of SNe 1987A and 1999em. In comparison with SN 2004et, dust formation in these two SNe occurred at much later phases, more than 400 d after the explosion.

4.2 $H\alpha$ Luminosity and Nickel Mass

During the nebular phase, the $H\alpha$ emission of the type II-P SNe is still very strong with respect to the continuum (e.g., see fig. 5 in Sahu et al. 2006). The bandwidth and center wavelength of the BATC i -band filter matches very well with the line profile of the $H\alpha$ emission; it is therefore likely to measure the $H\alpha$ luminosity through BATC i -band photometry. The continuum of the $H\alpha$ emission was measured from photometry in the BATC e -band (centered at $\sim 5000 \text{ \AA}$) which does not include contamination of any strong feature lines. Figures 4 and 5 show, respectively, the late-time evolution of the $H\alpha$ luminosity of SNe 2004dj ($0.55 \text{ dex } (100 \text{ d})^{-1}$) and 2004et ($0.60 \text{ dex } (100 \text{ d})^{-1}$) with no significant difference. In Figure 5, we also show the luminosity of the Ca II triplet ($\sim 8500 \text{ \AA}$) measured from BATC n -band photometry with a more rapid decline rate ($0.97 \text{ dex } (100 \text{ d})^{-1}$) than $H\alpha$. This may imply a dissimilar later-time mechanism or variational optical depths for these two emission lines which can be researched in detail by spectroscopic observations.

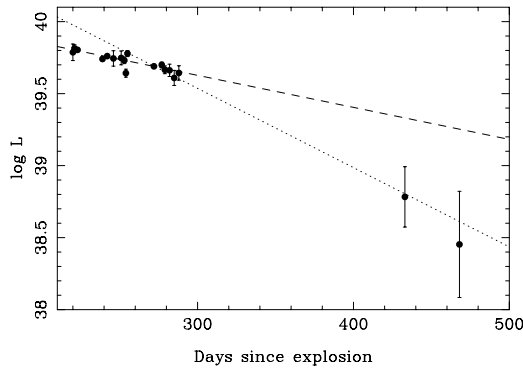


Fig. 4 Luminosity of $H\alpha$ of SN 2004dj.

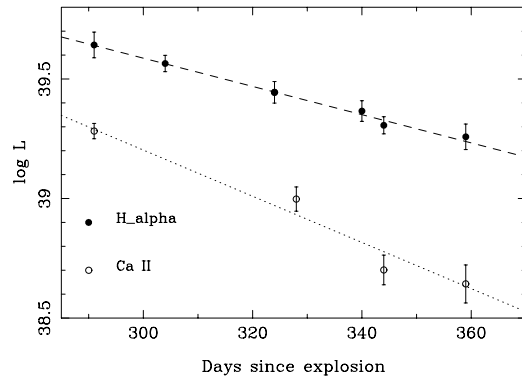


Fig. 5 Luminosity of $H\alpha$ and Ca II of SN 2004et.

As seen in the light curves, the linear evolution of the $H\alpha$ luminosity of SN 2004dj seems to break between $t \sim 300 - 400 \text{ d}$, though the two measurements after $t \sim 400 \text{ d}$ have large uncertainties. The observations of SN 2004dj by Tsvetkov et al. (2008), which continue to 3.5 yr, give a result that the light curves in the R and I -bands at later epochs are flatter than most SNe II-P. In any case, more observations of SNe II-P with late-time photometry spanning a few years after the explosion may help to give further constraints to the density model of matter around a supernova.

5 CONCLUSIONS

We present multi-band, late-time photometry of two nearby and bright II-P SNe, 2004dj and 2004et, extending to 1–1.5 yr after the explosion.

SN 2004dj exhibits a decline rate slightly slower than radioactive decay, with the decline rate $\beta \approx 0.7 \pm 0.1 \text{ mag } (100 \text{ d})^{-1}$. The flatter evolution during the earlier nebular phase is more likely to be related to the delayed recombination emission, though quantitative analysis is required for the energy produced by progenitors.

In comparison with the other sample of normal SNe II-P in our study, SN 2004et declines at the fastest pace during $t \sim 300 - 360$ d, e.g. $\beta \approx 1.3 \pm 0.1 \text{ mag } (100 \text{ d})^{-1}$. A similar feature was observed in SN 1987A and perhaps in SN 1999em, but at a much later phase (e.g., $t \approx 500$ d). Dust formation in the ejecta may be responsible for the steepening of the late-time evolution of their light curves.

Acknowledgements We are indebted to the referee for thoughtful comments and insightful suggestions that improved this paper greatly. This study has been supported by the Chinese National Natural Science Foundation through grants 10873016, 10803007, 10473012, 10573020, 10633020, 10603006 and 10673007, and by the National Basic Research Program of China (973 Program) No. 2007CB815403, the National Key Basic Research Science Foundation (NKBRSF TG199075402) and Basic Research Funding at Tsinghua University (JCqn2005036).

References

- Baron, E., et al. 2000, ApJ, 545, 444
Benetti, S., et al. 2001, MNRAS, 322, 361
Catchpole, R. M., et al. 1988, MNRAS, 231, 75p
Chevalier, R. A., & Fransson, C. 1992, ApJ, 395, 540
Elmhamdi, A., et al. 2003, MNRAS, 338, 939
Fan, X., et al. 1996, AJ, 112, 628
Fransson, C., et al. 2007, Msngr, 127, 44
Hamuy, M. 2003, ApJ, 582, 905
Hendry, M. A., et al. 2006, MNRAS, 369, 1303
Hendry, M. A., et al. 2005, MNRAS, 359, 906
Karachentsev, I. D., Karachentseva, V. E., Huchtmeier, W. K., & Makarov, D. I. 2004, AJ, 127, 2031
Leonard, D. C., et al. 2002, PASP, 114, 35
Leonard, D. C., et al. 2003, ApJ, 594, 247
Li, W., et al. 2005, PASP, 117, 121
Li, W., et al. 2007, ApJ, 661, 1013
Maíz-Apellániz, J., et al. 2004, ApJ, 615, L113
Nakano, S., Itagaki, K., Bouma, R. J., Lehky, M., & Hornoch, K. 2004, IAUC, 8377
Nugent, P., et al. 2002, PASP, 114, 803
Oke, J. B., & Gunn, J. E. 1983, ApJ, 266, 713
Pierce, M. J. 1994, ApJ, 430, 53
Sandage, A. 1984, AJ, 89, 630
Sahu, D. K., et al. 2006, MNRAS, 372, 1315
Schmidt, B. P., et al. 1992, ApJ, 395, 366
Schmidt, B. P., et al. 1993, AJ, 105, 2236
Schmidt, B. P., et al. 1994, ApJ, 432, 42
Smartt, S. J., et al. 2002, ApJ, 565, 1089
Smartt, S. J., et al. 2009, MNRAS, 395, 1409
Stetson, P. B. 1987, PASP, 99, 191
Tsvetkov, D. Y., et al. 2008, Peremennye Zvezdy, 28, 8
Turatto, M., et al. 1998, ApJ, 498, L129
Tully, R. B. 1988, Nearby Galaxy Catalog (Cambridge: Cambridge Univ. Press)
Vinkó, J., et al. 2006, MNRAS, 369, 1780
Wang, X. F., et al. 2005, ApJ, 626, L89
Wang, X. F., et al. 2008, ApJ, 675, 626
Weaver, T. A., & Woosley, S. E. 1980, AIPC, 63, 15
Yan, H., et al. 2000, PASP, 112, 691
Zhang, T., et al. 2004, AJ, 128, 1857
Zhang, T., et al. 2006, AJ, 131, 2245
Zhou, X., et al. 2003, A&A, 397, 361
Zwitter, T., Munari, U., & Moretti, S. 2004, IAUC, 8413